Available online at www.sciencedirect.com
SCIENCE DIRECT®
ELSEVIER
Nuclear Instruments and Methods in Physics Research B 217 (2004) 276–280
NIM B
Beam Interactions with Materials & Atoms
www.elsevier.com/locate/nimb

A description of bubble growth and gas release during thermal annealing of helium implanted copper

J.H. Evans [a,*], R. Escobar Galindo [b], A. van Veen [b]

[a] *Camrose Consultants, 27 Clevelands, Abingdon, Oxon OX14 2EQ, UK*
[b] *Interfaculty Reactor Institute, Delft University of Technology, Mekelweg 15, NL-2629 JB Delft, The Netherlands*

Received 9 June 2003; received in revised form 22 October 2003

Abstract

This paper describes an investigation into the migration and coalescence of equilibrium bubbles in helium implanted copper. Using computer simulation methods, the results indicate that when the swelling averaged over the implant depth approached 12%, the subsequent migration and coalescence leads to the unexpected formation of relatively massive bubbles with radii of the order of the helium range (~130 nm), some 10 times the average bubble radius. Such behaviour would appear to provide an explanation for the surface pores and the large helium loss during annealing observed in the experimental results of Escobar Galindo et al. [Nucl. Instr. and Meth. B, in press].

1. Introduction

In a recent paper, Escobar Galindo et al. [1] described the surface phenomena seen on copper implanted with 30 keV helium ions to doses of 1.2, 1.8 and 2.4×10^{16}/cm^2 and then annealed to 973 K for 1800 s. The mean range of the implanted helium was 130 ± 57 nm while for the highest dose the helium concentration at the peak was ~1.68 at.%. The study included the implantation through fine microsieves and the potential application to thin layer adhesion measurements [2]. Of interest here were the results which showed than in implanted areas, among other effects, a uniform distribution of pinholes was apparent (Fig. 1).

For the whole range of helium doses investigated, scanning electron microscope observations showed their density to be of the order of 3/μm^2, with diameters around 150 nm. The presence of the pinholes suggested that relatively large subsurface bubbles of this size were present. Scanning electron microscopy images after surface removal using electropolishing were consistent with this picture as was the large loss of approximately 80% of the implanted helium. However, straightforward application of analytical expressions [3,4] for the average equilibrium bubble radii expected at the range peak after the 973 K annealing suggested that this would be only 14.0 nm for the highest dose [1]. A surface diffusion coefficient of 8×10^{-9} cm^2/s was used for this calculation, obtained from the results of Willertz and Shewmon [5] on annealing helium bubbles in copper at 973 K. It seemed clear that the predicted bubble size could

* Corresponding author. Tel./fax: +44-1235-525059.
E-mail address: jhevans@lineone.net (J.H. Evans).

0168-583X/$ - see front matter © 2003 Elsevier B.V. All rights reserved.
doi:10.1016/j.nimb.2003.10.013

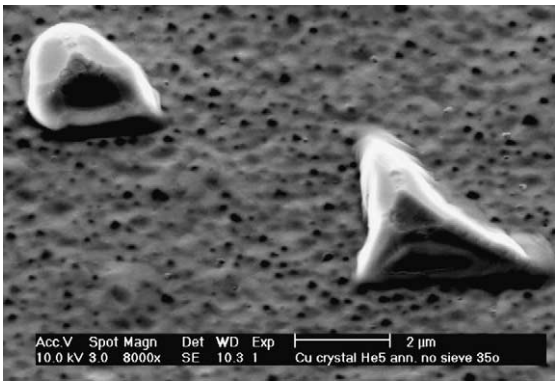

Fig. 1. Scanning electron micrograph showing the surface pinholes (dark spots) found in copper samples after annealing to 973 K for 1800 s [1].

not alone lead to the surface pinhole observations, nor to the large release fraction of the implanted helium.

In this paper, we describe a computer modelling approach, the results of which suggest that the formation of pinholes is a surprising but natural outcome of conventional migration and coalescence. The modelling simulated the random walk of bubbles during the annealing of an initial bubble distribution, allowing the migration and coalescence of the bubbles to be followed under thermal equilibrium conditions. While early times showed the expected relatively uniform coarsening of the bubble population as predicted analytically, eventually a sequence of seemingly unpredictable local coalescence events produced bubbles with radii some 10 times the average radius and some 1000 times the average volume. This breakaway swelling, together with the proximity of the surface, combine to provide a reasonable picture of the pinhole formation and gas release results reported by Escobar Galindo et al. [1].

2. Computer modelling

An initial population of 4000 bubbles was set up in a semi-infinite block within a program, with the helium bubble depth distribution following a Gaussian fit to the TRIM calculated distribution for 30 keV helium ions into copper. The size of the block was controlled by the choice of the initial bubble radius in order to fit the helium dose to be modelled. For the highest dose to be discussed in this paper, the starting radius was $r = 0.35$ nm, corresponding roughly with that expected in the initial ambient temperature implant. This value was based on the transmission electron microscopy results of Johnson and Mazey after helium implantation of copper [6], taking dose differences into account. To add variation, the starting radii were treated to give a Gaussian distribution of radii about the average. In the simulation of the high temperature anneal, spherical equilibrium bubbles were assumed, with coalesced bubbles immediately re-equilibrating to a new radius to maintain the usual $P = 2\gamma/r$ relation where P is the bubble pressure, r its radius and γ the surface energy. Since the aim of this work was to provide a qualitative rather than quantitative picture of the bubble behaviour, the calculations were simplified by using the ideal gas law to relate the bubble sizes with their helium content.

The model allowed individual bubbles to move randomly according to surface diffusion kinetics, using the bubble diffusion relation [7,8]

$$D_b = (3\Omega^{4/3})/(2\pi r^4)D_s, \quad (1)$$

where Ω is atomic volume of the matrix and D_s the surface diffusivity. In the calculations a value of 8×10^{-9} cm^2/s was used, as in [1] already mentioned in Section 1. Together with random walk theory, it is easy to show that for a bubble with radius r_i the jump step in a given time is proportional to $(1/r_i^2)$. After each jump step cycle in which all bubbles were moved, bubbles were tested against their near neighbours for touching and if so were allowed to coalesce to give a new bubble with a radius reflecting its new larger helium content. Because of the inverse relation of bubble pressure with radius, any coalescence under equilibrium bubble conditions leads, as is well known, to an increase in the vacancy to helium atom ratio and hence an increase in local swelling. Bubbles were also tested in position against the free surface. If they touched the surface, the helium was lost and, except when they were large (see later), the bubble removed. These procedures allowed the

accumulated gas loss and the bubble size parameters to be followed with time.

One problem with modelling coalescence events is that the process leads to a reduction in bubble numbers and therefore in statistics. In a recent simulation of Ostwald ripening of voids in silicon [9], an analogous problem was treated by using a cloning procedure. In the present case, after the bubble numbers were reduced by a factor of four from 4000 to 1000, the block was cloned and used to create an irradiated area a factor of four greater, thus returning to 4000 bubbles in the system. The depth remained as before so that both the depth and radius distributions were unchanged in the procedure. While the local spatial distributions of bubbles within the four quadrants were initially identical, their subsequent random movement quickly introduced differences. This iteration procedure could be repeated as many times as required.

3. Results

3.1. Bubble growth

During the first part of the 973 K anneal simulations, the bubble coarsening behaviour was much as expected, with a gradual coarsening of the bubble populations. However, on moving to longer times an unexpected but significant effect was seen. Quite rapidly, out of what appeared to be a typical cluster of bubbles, a large bubble was formed. The randomness of bubble movement meant that there were variations between the several computer runs to examine this effect but the qualitative results were always identical. In simulations of the highest experimental dose, 2.4×10^{16} 30 keV He^+/cm^2, the breakaway bubble growth took place between 400 and 600 s. An example is seen in Fig. 2 which shows a plan view of the bubble area at three different times. In a relatively short space of time, one group of bubbles in Fig. 2(a) have coalesced to form the individual large bubble seen in Fig. 2(b) with a radius an order of magnitude larger than the average, while in further annealing, more large bubbles are created to give the picture shown in Fig. 2(c) where they clearly dominate the substructure.

All the large bubbles observed were centred close to the helium peak thus defining their final radius values. This is seen in Fig. 3 where a 200 nm slice of the same volume as in Fig. 2 is observed in cross-section. The first two projections correspond to the times in Fig. 2(a) and (b), again illustrating the dramatic growth of the large bubble. Fig. 3(c) is at only a slightly longer time than in 3(b) showing the situation where the large bubble has grown further by local coalescence to touch the surface. At this point in the model, the bubble releases its gas.

The significance of the results in Figs. 2 and 3 is that we immediately have a plausible picture that leads to the formation of the surface pinholes seen experimentally, with the potential, as discussed in the next section, to considerably increase the total gas loss. The same bubble growth phenomenon

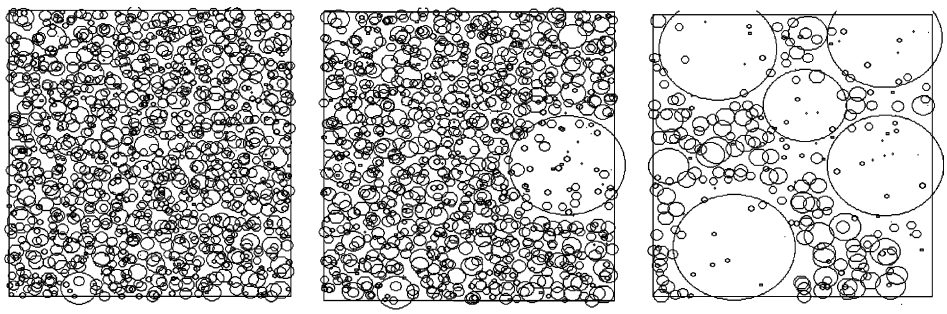

Fig. 2. Plan views of a 627×627 nm^2 bubble area drawn from the highest dose simulation data after annealing at 973 K for (a) 335, (b) 412 and (c) 1860 s.

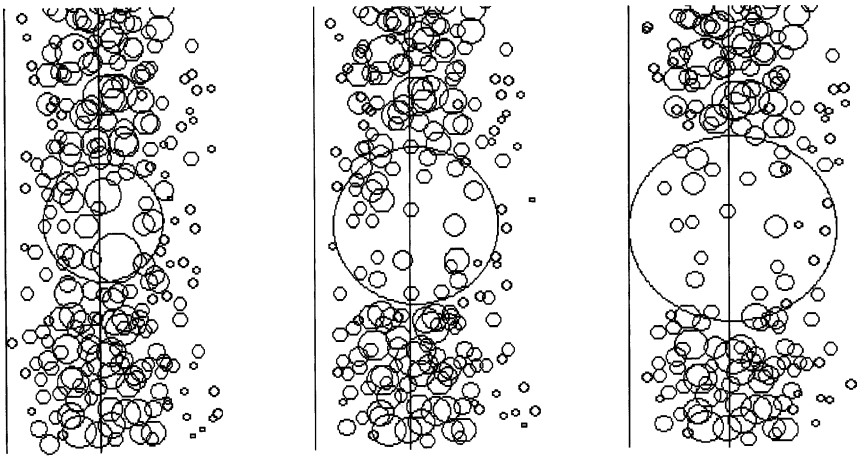

Fig. 3. Cross-sectional view following the formation of a large bubble; (a) and (b) are after annealing at 973 K for 335 and 412 s, respectively, using the same data as used for the plan view projections in Fig. 2(a) and (b). In (c), the annealing time is 447 s and shows the touching of the bubble at the sample surface. The central vertical line marks the original peak at a depth of 130 nm and acts here as a scale marker.

was seen for simulations of the medium dose helium implant over the experimental 1800 s timescale. However, for the lowest dose, times of an order of magnitude larger were necessary to initiate the formation of the first large bubble.

3.2. Gas release and swelling

In the modelling, any small bubbles reaching the surface were removed but the large bubbles more realistically were immobilised once they had intersected the surface. It seemed self-evident that these large bubbles must then act as large coalescence targets for the surrounding small bubbles, effectively increasing the sample surface area and thus creating an important additional route for the escape of helium, hugely increasing the amount of gas release. It was straightforward in the model to measure this quantity of gas as well as other parameters such as swelling, bubble radius and the root mean cube radius. It should be noted that the definition of swelling is arbitrary since there is a variation with depth arising from the original helium profile. Here it is defined as the average value over a depth twice the implanted range.

As already mentioned, the randomness of bubble movement meant that no two computer runs were identical, thus always giving small variations in the quantitative results. An example of the quantitative data, again for the highest dose simulation, is given in Fig. 4 where the swelling, gas loss and radius parameters are plotted as a function of time.

The formation of the first large bubble took place in all runs when the average swelling was in the region of 12%, although the swelling near the helium peak was well in excess of this. In Fig. 4 this point was reached near 550 s and was

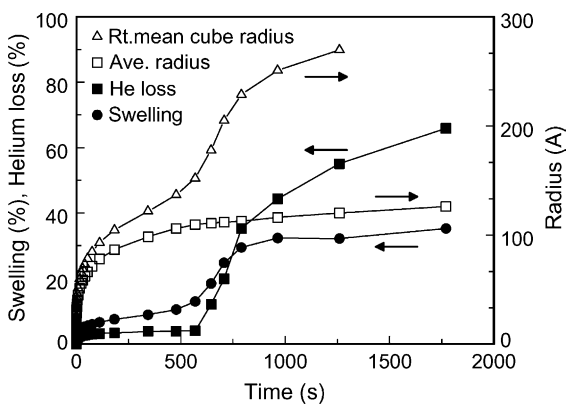

Fig. 4. Simulation results showing the changes in swelling, gas loss and radius parameters as a function of annealing time.

accompanied by a sharp rise in average swelling and gas loss and a marked deviation between the two radii values. The swelling continued to rise as more large bubbles formed but was then very much moderated by the large gas loss. This loss parameter had a moderate value (<5%) prior to the first large bubble intersecting the surface at which point it rose sharply followed by a large continuous increase as other large bubbles formed to act as the extra gas release route for the smaller bubbles. The total gas loss after 1800 s annealing varied from 65% to 80%, giving good qualitative agreement with that found experimentally. Of this gas loss, a very large fraction was released via the large bubbles thus emphasising the importance of this internal route for gas release.

It is worth noting that the variation of average bubble radius with time evolved much as expected. The average bubble size followed the analytical $(\text{time})^{1/5}$ behaviour [3,4,10] reasonably closely considering the perturbations that might be expected from the non-uniform helium concentration and the loss of helium at the surface.

4. Conclusions

The computer modelling results based on straightforward simulation of random bubble movement have provided a plausible picture of the experimental results reported in the preceding paper [1], in particular the large percentage loss of helium and the clear formation of surface pinholes. Clearly there are several assumptions in the modelling including the application of the ideal gas law, the accuracy of the Gaussian fit to the helium depth distribution, the availability of thermal vacancies and the instantaneous re-equilibration of bubbles. In addition, the phenomenon of bubble movement up the thermal vacancy gradient towards the surface as discussed by Evans and van Veen [11] has been ignored. Nevertheless, it is hard to see that any of the above assumptions could have affected the qualitative breakaway growth of the individual bubbles observed in the simulations. The fit of results with experiment strongly suggests that we are seeing a real (and novel) effect. It is interesting that extremely large bubbles are present at the end point of anneals in the work of Marachov et al. [12] on helium-implanted nickel.

From the point of view of quantitative behaviour, the computer simulations suggested that in both the medium and high helium doses, pinhole formation would have occurred on the experimental timescale (1800 s). However, there was a strong dependence on helium concentration and much longer times were predicted for the pinhole formation for the lowest helium dose. One reason might be that the surface diffusivity, although an experimental value, was too low. The possibility that the ideal gas assumption might explain the results was checked. For a fixed gas atoms/bubble value, it gives a smaller radius than a more acceptable equation of state (e.g. Mills et al. [13]) or using the van der Waals equation. As a result, in the simulation the bubbles will move faster than might be expected in practice and thus shorten the time required for the breakaway swelling to start. This does not help the lowest dose result. Further experimental work examining the evolution of the pinholes with time would clearly be useful.

References

[1] R. Escobar Galindo, A. van Veen, J.H. Evans, H. Schut, J.Th.M. de Hosson, Nucl. Instr. and Meth. B, in press. doi:10.1016/j.nimb.2003.10.012.
[2] R. Escobar Galindo, A. van Veen, J.H. Evans, H. Schut, J.Th.M. de Hosson, ICMCTF 2003, San Diego, Thin Solid Films, in press.
[3] E.E. Gruber, J. Appl. Phys. 38 (1967) 243.
[4] P.J. Goodhew, S.K. Tyler, Proc. Roy. Soc. A 377 (1981) 151.
[5] L.E. Willertz, P.G. Shewmon, Metall. Trans. 1 (1970) 2217.
[6] P. Johnson, D.J. Mazey, J. Nucl. Mater. 127 (1985) 30.
[7] R. Kelly, Phys. Status Solidi 21 (1967) 451.
[8] F.A. Nichols, J. Nucl. Mater. 30 (1969) 143.
[9] J.H. Evans, Nucl. Instr. and Meth. B 196 (2002) 125.
[10] H. Schroeder, P.F.P. Fichtner, H. Trinkaus, in: S.E. Donnelly, J.H. Evans (Eds.), Fundamental Aspects of Inert Gases in Solids, Plenum Press, New York, 1991, p. 289.
[11] J.H. Evans, A. van Veen, J. Nucl. Mater. 233–237 (1996) 1179.
[12] N. Marachov, L.J. Perryman, P.J. Goodhew, J. Nucl. Mater. 149 (1987) 296.
[13] R.L. Mills, D.H. Liebenberg, J.C. Bronsen, Phys. Rev. B 21 (1980) 5137.